Journal of Electroanalytical Chemistry 632 (2009) 45–54

Contents lists available at ScienceDirect

Journal of Electroanalytical Chemistry

journal homepage: www.elsevier.com/locate/jelechem

A comparative study of anodic fluorination of *N*-alkyl and *N,N*-dialkyl phenylacetamides in $Et_3N \cdot 4HF$ medium

N. Ilayaraja, M. Noel *

Electro Organic Division, Central Electrochemical Research Institute (CSIR), Karaikudi 630 006, India

ARTICLE INFO

Article history:
Received 2 January 2009
Received in revised form 25 March 2009
Accepted 26 March 2009
Available online 1 April 2009

Keywords:
Anodic fluorination
N-alkyl phenylacetamide
N,N-dialkyl phenylacetamide
$Et_3N \cdot 4HF$
Nuclear fluorination

ABSTRACT

Anodic fluorination of *N*-alkyl and *N,N*-dialkyl phenylacetamides (alkyl = methyl, ethyl, propyl and *n*-butyl) was carried out in $Et_3N \cdot 4HF$ medium. Effects of current density, quantity of electric charge and alkyl chain length on the overall conversion efficiency and selectivity of fluorinated products are reported. ^1H NMR, ^{19}F NMR and GC/MS were employed for product identification and characterization. Under galvanostatic condition, *N*-alkyl phenylacetamides lead to predominantly monofluoro derivative at ortho position in the aromatic ring. Mono and difluoro active methylene derivatives and *p*-fluoro compounds were also formed in smaller quantities. The selectivity was low in the case of *N,N*-dialkyl phenylacetamides. On increasing the electricity passed beyond 2 F/mol, the *o*-fluoro compound produced 1,4 addition compounds followed by further chemical and electrochemical transformations. Cyclic voltammetric studies indicated significant adsorption of *N,N*-dialkyl compounds. Potentiostatic electrolysis lead to predominantly side chain fluorination at the active methylene group. The product distribution under different experimental conditions is explained on the basis of reactant adsorption and protonation at the amide group.

1. Introduction

Anodic fluorination of aromatic and heterocyclic compounds in the absence and presence of aprotic solvents containing ionic liquids such as $Et_4NF \cdot mHF$ and $Et_3N \cdot nHF$ has received considerable attention in recent times. These developments have been reviewed from time to time in this laboratory [1,2] and elsewhere [3–5]. A broad perspective on the mechanistic aspects of electrochemical perfluorination and selective fluorination process has also been documented [6].

Selective nuclear fluorination in the aromatic and hetero cyclic rings as well as in the side chain containing active methylene group ($-CH_2-$) has been a major objective in the anodic fluorination studies. It is well established that the $-CH_2-$ group attached to the sulfur atom can undergo anodic fluorination with ease and high selectivity. Fuchigami et al. have carried out extensive work on different sulfur containing $-CH_2-$ compounds [3,5,7–9]. Effects of adsorption [10] and different solvents [11] on the anodic fluorination of sulfur compounds have been reported from this laboratory. In a similar manner, $-CH_2-$ group attached to selenium exhibits good selectivity towards electrochemical fluorination [12].

Laurent et al. have patented anodic fluorination of side chain $-CH_2-$ containing esters and amides [13,14]. Stereo selectivity in such processes has also been reported for esters and amides [15,16]. Anodic fluorination of alkyl phenylacetates was studied by Yoneda et al. in dichloromethane containing $Et_3N \cdot nHF$, $Et_4NF \cdot mHF$ and $Et_4N \cdot BF_4$ [17]. Shainyan et al. employed anhydrous hydrofluoric acid for the anodic fluorination of benzamide and acetanilide [18]. Chemical fluorination can also be achieved by using halide exchange process [19] or by employing other novel fluorinating agents [20]. Solvent free $Et_3N \cdot nHF$ and $Et_4NF \cdot mHF$ has been successfully employed for anodic fluorination of compounds which are more difficult to fluorinate in presence of solvents [21,23,25–29].

In the present study, we have investigated the product distribution patterns of anodically fluorinated *N*-alkyl and *N,N*-dialkyl phenylacetamides in solvent free $Et_3N \cdot 4HF$ medium.

2. Experimental

2.1. Materials

Synthetic grade (>98%) phenylacetyl chloride, dibutylamine, dimethylamine and propylamine were purchased from M/s Merck, Germany and used without further purification. High pure (>99%) triethylamine, *n*-butylamine and ethylamine (70% in water) were purchased from Sisco Research Laboratory, India. Dipropylamine and methylamine (40% in water, Fluka AG Germany) and Diethylamine (Nice Chemicals, India) were employed without further

* Corresponding author. Tel.: +91 4565 227772; fax: +91 4565 227779.
E-mail address: yemenoel@yahoo.co.in (M. Noel).

0022-0728/$ - see front matter © 2009 Elsevier B.V. All rights reserved.
doi:10.1016/j.jelechem.2009.03.014

purification. Anhydrous hydrogen fluoride (AHF) >99.9% was obtained from M/s TANFAC, Cudalore, Tamilnadu, India. Preparation of $Et_3N \cdot 4HF$ has been reported elsewhere [21].

2.2. Preparation of 2-phenylacetamide

Acyl chloride (0.035 M) was added drop-wise to a well stirred concentrated aqueous ammonia (20 ml) cooled in a freezing ice salt mixture to obtain a white precipitate of 2-phenylacetamide. The amide was filtered, dried and recrystallized using hot ethanol. The yield and purity of 2-phenylacetamide is 83% and >98%, respectively.

2.3. Preparation of N-alkyl and N,N-dialkyl phenylacetamides

An ice cold solution of 0.035 M phenylacetyl chloride was added to a beaker containing 40 ml of 10% NaOH and 0.03 M methylamine. The mixture was stirred well for about an hour. A white precipitate of *N*-methyl phenylacetamide was obtained. The amide was filtered and dried. The amide thus obtained was recrystallised using hot ethanol. Similar procedure was followed for the preparation of other *N*-alkyl and *N*,*N*-dialkyl phenylacetamides. The yield obtained for *N*-alkyl phenylacetamides and *N*,*N*-dialkyl phenylacetamides was 80–85% and 74–82%, respectively. The purity was checked by HPLC and found to be >98%.

2.4. Cyclic voltammetry and potentiostatic electrolysis

Cyclic voltammetry was carried out using an undivided polypropylene cell. The working electrodes were glassy carbon (0.07 cm^2) and platinum (0.07 cm^2). The counter electrode was a smooth platinum foil (1 cm^2) and the reference electrode was a palladium wire. Prior to the experiments, the glassy carbon electrode was polished with 4/0 emery sheet using alumina gel (0.05 μm) and washed with distilled water. Further, the electrode was sonicated for 5 min to remove any adsorbed alumina particles. $Et_3N \cdot 4HF$ was pre-electrolysed at a constant cell voltage of 2.5 V under nitrogen atmosphere to remove moisture and deaerated for 15 min with nitrogen gas to eliminate interfering oxygen before the start of the experiment.

For comparison, anodic fluorination of *N*-ethyl phenylacetamide and *N*,*N*-diethyl phenylacetamide was also carried out under potentiostatic condition, where working and counter electrodes were smooth platinum foil (1 × 3 cm^2) and palladium wire was used as reference electrode.

2.5. Electrochemical fluorination

Undivided polypropylene tube (5 ml) was served as a preparative cell for the anodic fluorination of *N*-alkyl and *N*,*N*-dialkyl phenylacetamides. The anode and cathode were a rectangular platinum foil (1 × 3 cm^2). Pre-electrolysis of 5 ml of $Et_3N \cdot 4HF$ solution was carried out at a constant cell voltage of 2.5 V under nitrogen atmosphere. The corresponding current density was around 1.5 mA/cm^2 at the start of pre-electrolysis and dropped to 20% of initial value (0.3 mA/cm^2) after 90 min. The reactant (*N*-alkyl or *N*,*N*-dialkyl phenylacetamides, 0.3 mol) was added subsequently and the electrolysis was carried out galvanostatically using an in-house fabricated galvanostat at 25 ± 2 °C. After completion of electrolysis, the electrolyte was mixed with 50 ml of cold water and extracted using diethyl ether. The extract was washed with brine solution and dried over anhydrous magnesium sulfate. The ether was distilled and the products were characterized using ^1H NMR, ^{19}F NMR and GC/MS.

2.6. Equipments

The purity of the reactant samples was checked by HPLC (Shimadzu 10VP) with ODS column using UV–Visible detector (254 nm). Methanol–water mixture (70:30) was used as eluent. ^1H NMR spectra were recorded with 400 MHz Bruker NMR Spectrometer with $CDCl_3$ and TMS as solvent and reference, respectively. ^{19}F NMR (376.5 MHz) of the products was recorded using $CFCl_3$ as internal reference. The products dissolved in chloroform

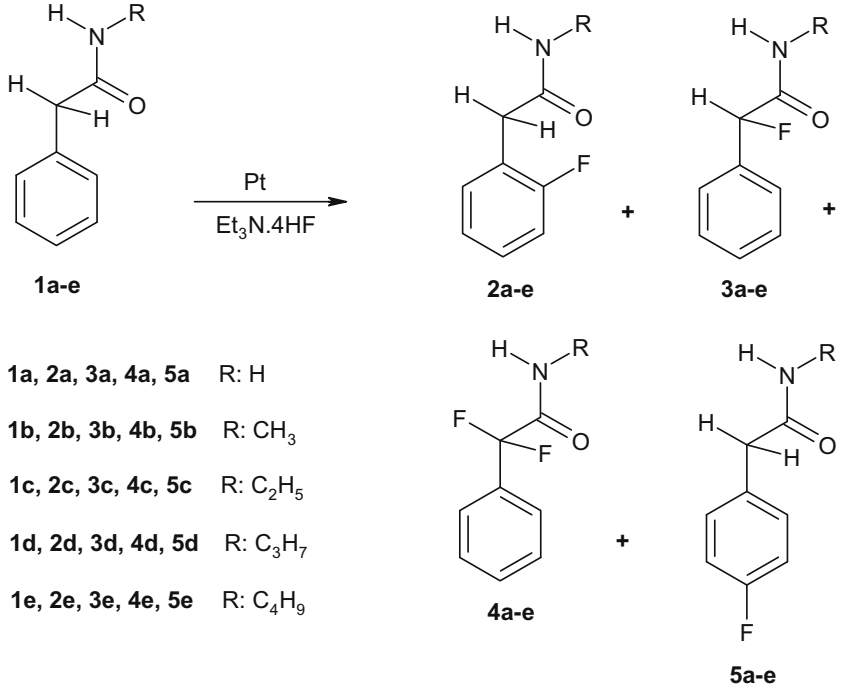

Scheme 1. Anodic fluorination pathway of *N*-alkyl phenylacetamides.

Table 1
^{19}F and ^{1}H NMR data of fluorinated *N*-alkyl phenylacetamides and its derivatives obtained during anodic fluorination of **1a–e** [21,22,24,27].

Reactants	Products			
	2a–e	**3a–e**	**4a–e**	**5a–e**
1a	−123.75 (q, 1F) $^{4}J_{HF}$ = 7.50 Hz	−174.50 (d, 1F) $^{2}J_{HF}$ = 48.90 Hz 5.78 (d, 1H) $^{2}J_{HF}$ = 48.20 Hz	−99.00 (s, 2F)	−117.47 (m, 1F)
1b	−124.36 (q, 1F) $^{4}J_{HF}$ = 7.53 Hz	−177.60 (d, 1F) $^{2}J_{HF}$ = 48.19 Hz 5.81 (d, 1H) $^{2}J_{HF}$ = 48.40 Hz	−98.93 (s, 2F)	−117.09 (m, 1F)
1c	−125.28 (q, 1F) $^{4}J_{HF}$ = 5.27 Hz	−176.56 (d, 1F) $^{2}J_{HF}$ = 48.19 Hz 5.76 (d, 1H) $^{2}J_{HF}$ = 47.60 Hz	−98.76 (s, 2F)	−117.19 (m, 1F)
1d	−123.75 (m, 1F)	−176.46 (d, 1F) $^{2}J_{HF}$ = 48.57 Hz $^{2}J_{HF}$ = 49.60 Hz 5.76 (d, 1H)	−98.84 (s, 2F)	−117.17 (m, 1F)
1e	−125.75 (q, 1F) $^{4}J_{HF}$ = 7.50 Hz	−177.05 (d, 1F) $^{2}J_{HF}$ = 48.90 Hz $^{2}J_{HF}$ = 48.80 Hz 5.78 (d, 1H)	−99.35 (s, 2F)	−117.67 (m, 1F)

were subjected to GC/MS analysis using Agilent 5975C GC/MSD with Triple-Axis HED-EM detector and 7890A GC. Cyclic voltammetry and potentiostatic studies were carried out using BAS IM6 Electrochemical Analyser (USA) and Thales 3.18-USB software.

3. Results and discussion

3.1. Galvanostatic fluorination of *N*-alkyl phenylacetamides

During the anodic fluorination of 2-phenylacetamide (**1a**) and *N*-alkyl phenylacetamides (**1b–e**) four major products were invariably obtained (Scheme 1). ^{1}H and ^{19}F NMR data for these four products are presented in the Table 1 reports [21,22,24,27]. The product mixture obtained from the anodic fluorination of **1b** was subjected to GC/MS analysis to distinctly identify the major products (**2b**, **3b** and **4b**) and the fragmentation pattern clearly indicated the formation of all these products (Table 2). The fluorine signals at −123 to −125 ppm with $^{4}J_{HF}$ value between 5 and 7.5 Hz correspond to *o*-fluoro derivatives (compounds **2a–e**). Similarly, the ^{1}H and ^{19}F NMR signals occurring at 5.78–5.81 ppm and −174 to −177 ppm, respectively (with $^{2}J_{HF} > 46$ Hz) belong to mono fluorinated side chain active methylene group, respectively (compounds **3a–e**). The fluorine signals for difluoro compounds (**4a–e**) and *p*-fluoro derivatives (**5a–e**) are at −98 to −100 ppm and −117 ppm, respectively. The product distribution pattern obtained for each of these compounds **1a–e** was calculated by quantitative analysis of integral data of ^{19}F NMR signals. The influence of anodic current density, total quantity of electric charge passed and alkyl substituents was evaluated by this procedure.

The influence of current density on the product distribution pattern of *N*-methyl phenylacetamide was investigated and the results are summarized in Table 3. In general, conversion efficiencies of

Table 2
GC/MS data of fluorinated products obtained during anodic fluorination of **1b** and **6a**.

Compound	GC/MS: m/z:
2b	167 ($[M]^{\cdot+}$, $C_9H_{10}FNO$, 24%); 152 ($[M-CH_3]^+$, C_8H_7NO, 18%); 151 ($[M-O]^{\cdot+}$, $C_9H_{10}FN$, 5%); 148 ($[M-F]^+$, $C_9H_{10}NO$, 8%); 137 ($[M-NH(CH_3)]^+$, C_8H_6FO, 11%); 109 ($[M-CO-NH(CH_3)]^+$, C_7H_6F, 48%); 95 ($[C_6H_4F]^+$, 7%); 72 ($[C_3H_6NO]^+$, 5%); 58 ($[C_2H_4NO]^+$, 100%); 30 ($[CH_4N]^+$, 20%)
3b	167 ($[M]^{\cdot+}$, $C_9H_{10}FNO$, 27%); 152 ($[M-CH_3]^+$, C_8H_7FNO, 17%); 148 ($[M-F]^+$, $C_9H_{10}NO$, 5%); 137 ($[M-NH(CH_3)]^+$, C_8H_6FO, 15%); 109 ($[M-CO-NH(CH_3)]^+$, C_7H_6F, 48%); 90 ($[C_3H_5FNO]^+$); 77 ($[C_6H_5]^+$, 29); 58 ($[C_2H_4NO]^+$, 100%); 30 ($[CH_4N]^+$, 10%)
4b	185 ($[M]^{\cdot+}$, $C_9H_9F_2NO$, 28%); 170 ($[M-CH_3]^+$, $C_8H_6F_2NO$, 12%); 166 ($[M-F]^+$, C9H9FNO, 6%); 155 ($[M-NH(CH_3)]^+$, $C_8H_5F_2O$, 11%); 127 ($[M-CO-NH(CH_3)]^+$, $C_7H_5F_2$, 26%); 108 ($[C_3H_4F_2NO]^+$, 5%); 77 ($[C_6H_5]^+$, 26%); 58 ($[C_2H_4NO]^+$, 100%); 30 ($[CH_4N]^+$, 22%)
7a	181 ($[M]^{\cdot+}$, $C_{10}H_{12}FNO$, 25%); 166 ($[M-CH_3]^+$, C_9H_9FNO, 4%); 165 ($[M-O]^{\cdot+}$, $C_{10}H_{12}FN$, 7%); 162 ($[M-F]^+$, $C_{10}H_{12}NO$, 2%); 137 ($[M-N(CH_3)_2]^+$, C_8H_6FO, 6%); 109 ($[M-CO-N(CH_3)_2]^+$, C_7H_6F, 55%); 104 ($[C_4H_7FNO]^+$, 6%); 77 ($[C_6H_5]^+$, 36%); 72 ($[C_3H_6NO]^+$, 100%); 44 ($[C_2H_6N]^+$, 27%)
8a	181 ($[M]^{\cdot+}$, $C_{10}H_{12}FNO$, 19%); 166 ($[M-CH_3]^+$, C_9H_9FNO, 9%); 165 ($[M-O]^{\cdot+}$, $C_{10}H_{12}FN$, 15%); 162 ($[M-F]^+$, $C_{10}H_{12}NO$, 5%); 137 ($[M-N(CH_3)_2]^+$, C_8H_6FO, 26%); 129 ($[C_6H_8FNO]^+$, 27%); 109 ($[M-CO-N(CH_3)_2]^+$, C_7H_6F, 27%); 95 ($[C_6H_4F]^+$, 12%); 86 ($[C_4H_8NO]^+$, 21%); 72 ($[C_3H_6NO]^+$, 100%); 44 ($[C_2H_6N]^+$, 32%)
9a	199 ($[M]^{\cdot+}$, $C_{10}H_{11}F_2NO$, 21%); 184 ($[M-CH_3]^+$, $C_9H_8F_2NO$, 11%); 183 ($[M-O]^{\cdot+}$, $C_{10}H_{11}F_2N$, 5%); 180 ($[M-F]^+$, $C_{10}H_{11}FNO$, 5%); 155 ($[M-N(CH_3)_2]^+$, $C_8H_5F_2O$, 11%); 147 ($[C_6H_7F_2NO]^+$, 7%); 127 ($[M-CO-N(CH_3)_2]^+$, $C_7H_5F_2$, 10%); 104 ($[C_4H_7FNO]^+$, 29%); 95 ($[C_6H_4F]^+$, 8%); 72 ($[C_3H_6NO]^+$, 100%); 44 ($[C_2H_6N]^+$, 20%)
11a	199 ($[M]^{\cdot+}$, $C_{10}H_{11}F_2NO$, 20%); 184 ($[M-CH_3]^+$, $C_9H_8F_2NO$, 5%); 183 ($[M-O]^{\cdot+}$, $C_{10}H_{11}F_2N$, 5%); 180 ($[M-F]^+$, $C_{10}H_{11}FNO$, 8%); 155 ($[M-N(CH_3)_2]^+$, $C_8H_5F_2O$, 21%); 127 ($[M-CO-N(CH_3)_2]^+$, $C_7H_5F_2$, 8%); 122 ($[C_4H_6F_2NO]^+$, 11%); 77 ($[C_6H_5]^+$, 14%); 72 ($[C_3H_6NO]^+$, 100%); 50 ($[CF_2]^{\cdot+}$, 25%); 44 ($[C_2H_6N]^+$, 37%)

Table 3
Effect of current density on the anodic fluorination of *N*-methyl phenylacetamide (**1b**).

Current density (mA/cm^2)	Conversion[a] (%)	Selectivity[b] (mol%)					
		2b	**3b**	**4b**	**5b**	Total CHF[c] groups	Others[d]
2.5	63.2	33.1	30.5	6.9	6.2	39.8	14.0
5	72.4	44.7	34.2	4.7	6.0	40.8	3.8
10	76.4	39.5	39.0	3.4	6.0	44.0	7.1
15	79.7	41.1	31.3	3.3	6.9	42.6	6.1

Electricity passed = 2 F/mole.
[a] Based on HPLC data.
[b] Based on NMR data.
[c] CHF signals observed in the region −174 to −184 ppm including **3a–e**.
[d] Other products include compounds **14–20**.

Table 4
Effect of charge on the anodic fluorination of *N*-methyl phenylacetamide (**1b**).

Charge passed (F/mol)	Conversion[a] (%)	Selectivity[b] (mol%)					
		2b	**3b**	**4b**	**5b**	Total CHF[c] groups	Others[d]
2	79.7	41.1	31.3	3.3	6.9	42.6	6.1
3	84.5	38.2	33.2	11.3	5.5	37.2	7.8
4	87.2	23.9	35.4	19.8	4.4	36.4	15.5
5	89.5	14.3	23.8	26.5	6.9	29.8	22.5
6	90.5	6.0	20.5	35.5	3.0	26.6	28.9

Current density = 15 mA/cm^2.
[a] Based on HPLC data.
[b] Based on NMR data.
[c] CHF signals observed in the region −174 to −184 ppm including **3b**.
[d] Other products include compounds **14**–**20**.

Table 5
Effect of chain length on the anodic fluorination of *N*-alkyl phenylacetamides (**1a**–**e**).

Run	Reactants	Conversion[a] (%)	Selectivity[b] (mol%)					
			2a–e	**3a–e**	**4a–e**	**5a–e**	Total CHF[c] groups	Others[d]
1	**1a**	82.0	21.2	48.2	18.2	3.3	53.1	4.2
2	**1b**	79.6	41.1	31.3	3.3	6.9	42.6	6.1
3	**1c**	81.5	41.5	25.8	8.9	5.1	37.4	7.1
4[e]	**1c**	89.0	15.0	41.7	1.3	5.8	51.9	26.0
5	**1d**	85.8	45.1	21.0	11.7	3.6	33.4	6.2
6[e]	**1d**	92.0	18.4	39.7	6.9	6.7	46.7	21.3
7	**1e**	86.5	40.3	20.1	19.0	3.5	30.4	6.8
8[e]	**1e**	93.4	19.6	38.4	7.2	6.9	45.6	20.7

Current density = 15 mA/cm^2.
Cell voltage = 2.83 − 2.95 V.
Electricity passed = 2 F/mole.
[a] Based on HPLC data.
[b] Based on NMR data.
[c] CHF signals observed in the region −174 to −184 ppm including **3a–e**.
[d] Other products include compounds **14**–**20**.
[e] Potentiostatic electrolysis at 2.2 V.

60–80% could be achieved by passing 2 F/mol of electric charge at different current densities. The conversion efficiency was less (63%) at a current density of 2.5 mA/cm^2. The *o*-fluoro derivative appears to be the main fluorinated product with 33–45% selectivity. Mono fluorination of side chain active methylene group was identified as the next major fluorination process. The main signal for this –CHF– group showed 30–39% selectivity. The total intensity of fluorine signals in the –CHF– region is higher (Table 3–5) than the other signals obtained in this region and this can be correlated with simultaneous nuclear fluorination apart from the side chain fluorination process. The total selectivity data corresponding to all –CHF– signals are also given in Table 3. The selectivity of side chain difluoro methylene product varied between 3% and 7% and the yield of *p*-fluoro derivative was 6–7%.

The influence of total quantity of electric charge passed on the product selectivity during the anodic fluorination of *N*-methyl phenylacetamide was also studied. Different electric charges ranging from 2 to 6 F/mol were passed at a current density 15 mA/cm^2 and the results are given in Table 4. The conversion efficiency increased from 80% to 90% with increasing quantity of electric charge passed. Considerable increase in the formation of difluoro methylene derivative was noticed with corresponding decrease in the –CHF– function when more than 3 F/mol of electric charge was passed. The selective formation of *o*-fluoro derivative was also found to decrease sharply with simultaneous increase in the evolution of other products. The selectivity of *p*-fluoro derivative was found to be low in all the cases.

The alkyl groups present in the *N*-alkyl phenylacetamides also influence the product distribution pattern as shown in Table 5. Side chain fluorination leading to the –CHF– derivative formation exhibited 48% selectivity for the parent compound **1a**. The selectivity consistently decreased with increase in alkyl chain length of the *N*-alkyl phenylacetamides. Simultaneously, the selectivity of *o*-fluoro derivative increased from 21% for **1a** to 45% for **1d**.

3.2. Galvanostatic fluorination of N,N-dialkyl phenylacetamides

Anodic fluorination of *N*,*N*-dialkyl phenylacetamides was also carried out under similar conditions described in Section 3.1. In this case, however, some interesting selectivity trends were noticed as shown in Scheme 2. The compounds **6a–d** produced side chain fluorinated (**7a–d**) and ortho fluorinated (**8a–d**) compounds in moderate yield. Further fluorination of **7a–d** and **8a–d** lead to **10a–d** and **9a–d**, respectively. Compounds **9** and **10** are the major difluoro derivatives obtained during the fluorination process. Fairly small quantities of side chain difluoro methylene compounds **11a–d** and *p*-fluoro compounds **12a–d** were also obtained under galvanostatic conditions. In the case of **6a**, one of the major product was *o*,*p* difluoro derivative (**13a**). The ^{1}H and ^{19}F NMR signals corresponding to the fluorinated products **7–13** are summarized in Table 6 and GC/MS data for **7a**, **8a**, **9a** and **11a** are presented in Table 2.

Typical results obtained during the electrochemical fluorination of **6a** at different current densities are given in Table 7. The overall

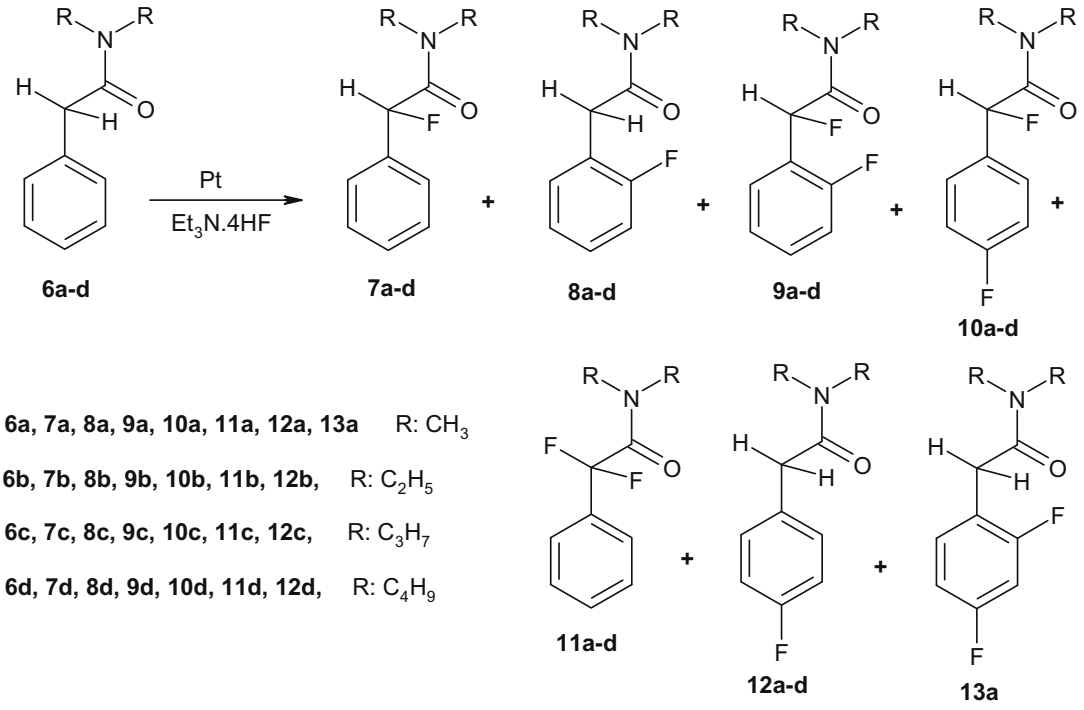

Scheme 2. Anodic fluorination pathway of *N*,*N*-dialkyl phenylacetamides.

Table 6
^{19}F and ^{1}H NMR data of fluorinated *N*,*N*-dialkyl phenylacetamides and its derivatives obtained during anodic fluorination of **6a–d**.

Reactants	Products						
	7a–d	**8a–d**	**9a–d**	**10a–d**	**11a–d**	**12a–d**	**13a**
6a	−177.94 (dd, 1F) $^{2}J_{HF}$ = 48.20 Hz $^{4}J_{HF}$ = 3.01 Hz 5.81 (d, 1H) $^{2}J_{HF}$ = 47.75 Hz	−124.29 (m, 1F)	−177.72 (d, 1F) $^{2}J_{HF}$ = 47.40 Hz 6.36 (d, 1H) $^{2}J_{HF}$ = 46.99 Hz −125.07 (m, 1F)	−172.90 (d, 1F) $^{2}J_{HF}$ = 49.30 Hz 6.07 (d, 1H) $^{2}J_{HF}$ = 49.27 Hz −117.43 (m, 1F)	−99.07 (s, 2F)	−117.51 (m, 1F)	−124.77 (m, 1F) −117.37 (m, 1F)
6b	−177.26 (dd, 1F) $^{2}J_{HF}$ = 48.50 Hz $^{4}J_{HF}$ = 2.25 Hz 5.65 (d, 1H) $^{2}J_{HF}$ = 50.10 Hz	−125.07 (m, 1F)	−177.11 (d, 1F) $^{2}J_{HF}$ = 47.90 Hz 6.32 (d, 1H) $^{2}J_{HF}$ = 47.81 Hz −124.03 (m, 1F)	−172.37 (d, 1F) $^{2}J_{HF}$ = 52.70 Hz 5.98 (d, 1H) $^{2}J_{HF}$ = 47.52 Hz −117.44 (m, 1F)	−99.37 (s, 2F)	−117.64 (m, 1F)	
6c	−177.14 (dd, 1F) $^{2}J_{HF}$ = 48.40 Hz $^{4}J_{HF}$ = 5.20 Hz 5.80 (d, 1H) $^{2}J_{HF}$ = 47.81 Hz	−125.10 (m, 1F)	−177.00 (d, 1F) $^{2}J_{HF}$ = 46.50 Hz 6.33 (d, 1H) $^{2}J_{HF}$ = 47.81 Hz −125.19 (m, 1F)	−171.83 (d, 1F) $^{2}J_{HF}$ = 48.90 Hz 6.04 (d, 1H) $^{2}J_{HF}$ = 50.62 Hz −117.41 (m, 1F)	−99.38 (s, 2F)	−117.67 (m, 1F)	
6d	−177.13 (dd, 1F) $^{2}J_{HF}$ = 48.90 Hz $^{4}J_{HF}$ = 3.50 Hz 5.79 (d, 1H) $^{2}J_{HF}$ = 47.81 Hz	−125.11 (m, 1F)	−176.87 (d, 1F) $^{2}J_{HF}$ = 47.80 Hz 6.32 (d, 1H) $^{2}J_{HF}$ = 47.81 Hz −125.76 (m, 1F)	−171.55 (d, 1F) $^{2}J_{HF}$ = 47.80 Hz 6.03 (d, 1H) $^{2}J_{HF}$ = 50.62 Hz −117.41 (m, 1F)	−99.37 (s, 2F)	−117.66 (m, 1F)	

Table 7
Effect of current density on the anodic fluorination of *N*,*N*-dimethyl phenylacetamide (**6a**).

Current density (mA/cm^2)	Conversion[a] (%)	Selectivity[b] (mol%)							
		7a	**8a**	**9a**	**10a**	**11a**	**12a**	**13a**	Others[c]
5	54.6	23.5	<1	18.5	<1	3.1	12.5	24.8	17.6
10	56.5	25.6	<1	20.9	<1	1.7	13.1	27.4	11.3
15	60.6	24.5	<1	23.4	<1	3.8	8.4	21.7	18.2

Electricity passed = 2 F/mole.
[a] Based on HPLC data.
[b] Based on NMR data.
[c] Other products include compounds **14–20**.

Table 8
Effect of charge on the anodic fluorination of *N*,*N*-dimethyl phenylacetamide (**6a**).

Charge passed (F/mole)	Conversion[a] (%)	Selectivity[b] (mol%)							
		7a	**8a**	**9a**	**10a**	**11a**	**12a**	**13a**	Others[c]
2	60.6	24.5	<1	23.4	<1	3.8	8.4	21.7	18.2
4	73.6	21.0	<1	19.4	<1	9.2	9.8	22.4	18.2
6	89.3	25.7	<1	10.6	<1	13.7	9.8	22.5	17.7

Current density = 15 mA/cm^2.
[a] Based on HPLC data.
[b] Based on NMR data.
[c] Other products include compounds **14**–**20**.

conversion efficiency at an electric charge of 2 F/mol varied from 54% to 60%. Compounds **7a**, **9a** and **13a** are the major products and the product distribution does not vary with current density.

It was found that the overall conversion efficiency can be enhanced by passing more than 2 F/mol of electric charge. Typical results obtained by passing different quantities of electric charge at a current density of 15 mA/cm^2 are presented in Table 8. The conversion efficiency improved from 60% to 90% when increasing the overall quantity of electric charge from 2 to 6 F/mol. Except for compounds **9a** and **11a**, the product distribution patterns of other compounds varied only slightly with different quantities of electric charge. The selectivity of compound **9a** decreased from 23% for 2 F/mol to 11% for 6 F/mol, which may be due to 2,3 or 2,5 addition reactions (Section 3.3, Scheme 3).

The effect of alkyl substituent on the selectivity and product distribution of *N*,*N*-dialkyl phenylacetamides is summarized in Table 9. With increase in the alkyl chain length, the conversion efficiency increased along with side chain monofluoro derivative (compound **7**). On the other hand, the difluoro derivative (**9**) decreased slightly with alkyl chain length without affecting the selectivity of other fluoro derivatives. The reason for the complete absence of *o*,*p* difluoro derivative in the case of **6b–d** is not clear. However, this experimental observation was repeatedly confirmed by experiments with different compounds at different conditions.

3.3. Other fluorinated products formed during galvanostatic fluorination of N-alkyl and N,N-dialkyl phenylacetamides

Apart from the fluorinated products indicated in Schemes 1 and 2, a few other low intensity fluorine signals were also observed in the ^{19}F NMR spectra. However, it is very difficult to identify these minor products. The total contributions from such products in each experiment are given in Tables 3–5 and 7–9. Significant increase in the yield of other products was noticed when more than 2 F/mol of electric charge was passed in the case of **1b** (Table 4). In both these cases **1b** and **6a**, simultaneous decrease in the selectivity of *o*-fluoro derivative was also noticed. Careful analysis of ^{19}F NMR signals of other products suggested chemical and electrochemical pro-

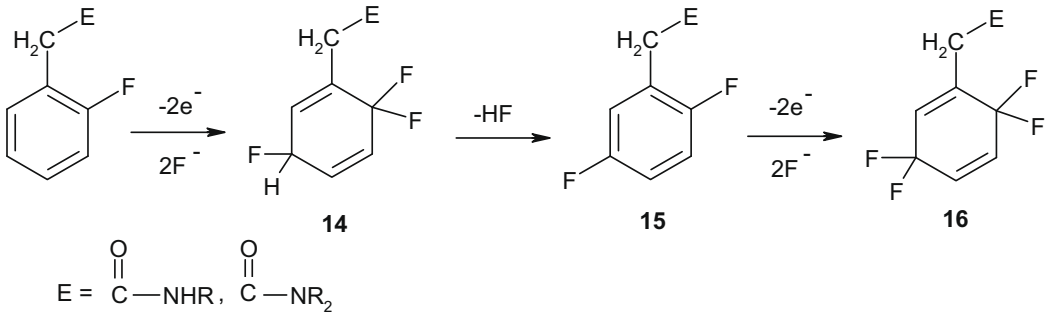

Scheme 3. Successive fluorination of *o*-fluoro alkyl phenylacetamides.

Table 9
Effect of chain length on the anodic fluorination of *N*,*N*-dialkyl phenylacetamides (**6a–d**).

Run	Reactants	Conversion[a] (%)	Selectivity[b] (mol%)							
			7a–d	**8a–d**	**9a–d**	**10a–d**	**11a–d**	**12a–d**	**13a**	Others[c]
1	**6a**	60.6	24.5	<1	23.4	<1	3.8	8.4	21.7	18.2
2	**6b**	64.6	26.1	31.2	14.6	17.6	4.6	4.5	–	1.4
3[d]	**6b**	85.0	53.9	5.1	6.1	<1	4.1	3.4	–	27.4
4	**6c**	72.9	32.0	28.0	11.9	15.7	5.5	1.2	–	5.7
5	**6d**	75.0	31.1	27.5	14.1	11.5	5.7	6.3	–	3.8

Electricity passed = 2 F/mole.
Cell voltage = 2.95 – 3.07 V.
Current density = 15 mA/cm^2.
[a] Based on HPLC data.
[b] Based on NMR data.
[c] Other products include compounds **14**–**20**.
[d] Potentiostatic electrolysis at 2.2 V.

Table 10
^{19}F NMR data of nuclear substitution and addition products [21–28].

No	Structure	Chemical shifts (δ, ppm)
14	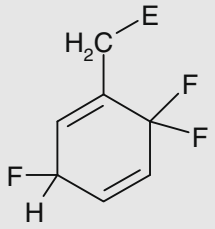	−184.88 (d, 1F) $^{2}J_{HF}$ = 46.68 Hz -97.93 (s, 1F) -98.64 (s, 1F) J_{AB} = 267 Hz
15	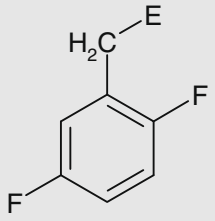	−125.48 (m, 1F) −124.09 (m, 1F)
16	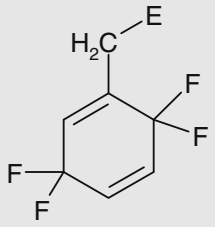	−100.86 (s, 2F) −95.54 (s, 2F)
17	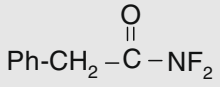	−14.57 (s, 2F)
18	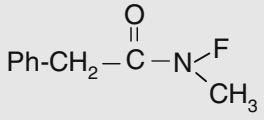	−100.86 (q, 1F) $^{3}J_{HF}$ = 3.77 Hz
19	Ph–CHF_2	−128.45 (d, 2F) $^{2}J_{HF}$ = 60.6 Hz
20	Ph–CH_2F	−221.23 (t, 1F) $^{2}J_{HF}$ = 51.60 Hz

Table 11
GC/MS data of fluorinated products obtained during anodic fluorination of **1b** and **6a**.

Compound	GC/MS: m/z:	
	E = C(O)–NH(CH_3)	E = C(O)–N(CH_3)$_2$
14	205 ([M]$^{\cdot+}$, $C_9H_{10}F_3NO$, 55%); 190 ([M−CH_3]$^+$, $C_8H_7F_3NO$, 2%);189 ([M−O]$^{\cdot+}$, $C_9H_{10}F_3N$, 6%); 186 ([M−F]$^+$, $C_9H_{10}F_2NO$, 8%); 175 ([M−NH(CH_3)]$^+$, $C_8H_6F_3O$, 20%); 147 ([M−CO–NH(CH_3)]$^+$,$C_7H_6F_3$, 100%); 133 ([$C_6H_4F_3$]$^+$, 24%); 72 ([C_3H_6NO]$^+$,60%); 58 ([C_2H_4NO]$^+$, 15%); 30 ([CH_4N]$^+$, 8%)	219 ([M]$^{\cdot+}$, $C_{10}H_{12}F_3NO$, 18%); 203 ([M−O]$^{\cdot+}$, $C_{10}H_{12}F_3N$, 5%); 200 ([M−F]$^+$, $C_{10}H_{12}F_2NO$, 7%); 175 ([M−N(CH_3)$_2$]$^+$, $C_8H_6F_3O$, 24%); 147 ([M−CO–N(CH_3)$_2$]$^+$, $C_7H_6F_3$, 35%); 133 ([$C_6H_4F_3$]$^+$, 20%); 86 ([C_4H_8NO]$^+$, 5%); 72 ([C_3H_6NO]$^+$, 100%); 44 ([C_2H_6N]$^+$, 29%)
15	185 ([M]$^{\cdot+}$, $C_9H_9F_2NO$, 15%); 170 ([M−CH_3]$^+$, $C_8H_6F_2NO$, 5%); 169 ([M−O]$^{\cdot+}$, $C_9H_9F_2N$, 5%); 166 ([M−F]$^+$, C_9H_9FNO, 12%); 155 ([M−NH(CH_3)]$^+$, $C_8H_5F_2O$, 4%); 127 ([M−CO–NH(CH_3)]$^+$, $C_7H_5F_2$, 22%); 113 ([$C_6H_3F_2$]$^+$, 8%); 101 ([$C_5H_2F_2$]$^+$, 5%); 72 ([C_3H_6NO]$^+$, 15%); 58 ([C_2H_4NO]$^+$,100%); 30 ([CH_4N]$^+$, 15%)	199 ([M]$^{\cdot+}$, $C_{10}H_{11}F_2NO$, 21%); 184 ([M−CH_3]$^+$, $C_9H_8F_2NO$, 8%);183 ([M−O]$^{\cdot+}$, $C_{10}H_{11}F_2N$, 8%); 180 ([M−F]$^+$, $C_{10}H_{11}FNO$, 7%); 155 ([M−N(CH_3)$_2$]$^+$, $C_8H_5F_2O$ 21%); 127 ([M−CO–N(CH_3)$_2$]$^+$,$C_7H_5F_2$, 20%); 113 ([$C_6H_3F_2$]$^+$, 21%); 86 ([C_4H_8NO]$^+$, 25%); 72 ([C_3H_6NO]$^+$, 100%); 44 ([C_2H_6N]$^+$, 37%)
16	223 ([M]$^{\cdot+}$, $C_9H_9F_4NO$, 15%); 208 ([M−CH_3]$^+$, $C_8H_6F_4NO$, 21%); 207 ([M−O]$^{\cdot+}$, $C_9H_9F_4N$, 40%); 193 ([M−NH(CH_3)]$^+$, $C_8H_5F_4O$, 29%); 165 ([M−CO–NH(CH_3)]$^+$, $C_7H_5F_4$, 8%); 151 ([$C_6H_3F_4$]$^+$, 20%); 147 ([$C_6H_7F_2NO$]$^{\cdot+}$, 36%); 72 ([C_3H_6NO]$^+$,100%); 58 ([C_2H_4NO]$^+$, 50%); 30 ([CH_4N]$^+$, 21%)	237 ([M]$^{\cdot+}$, $C_{10}H_{11}F_4NO$, 22%); 222 ([M−CH_3]$^+$, $C_9H_8F_4NO$, 5%); 221 ([M−O]$^{\cdot+}$, $C_{10}H_{11}F_4N$, 5%); 193 ([M−N(CH_3)$_2$]$^+$, $C_8H_5F_4O$, 48%); 165 ([M−CO–N(CH_3)$_2$]$^+$, $C_7H_5F_4$, 79%); 161 ([$C_7H_9F_2NO$]$^{\cdot+}$, 9%); 151 ([$C_6H_3F_4$]$^+$, 9%); 86 ([C_4H_8NO]$^+$, 9%); 72 ([C_3H_6NO]$^+$, 100%); 44 ([C_2H_6N]$^+$, 25%)

cesses involving *o*-fluoro derivative as indicated in Scheme 3. The ^{19}F NMR and GC/MS data corresponding to compounds **14–16** are summarized in Tables 10 and 11. Similar 1,4 addition of *o*-fluoro derivative was observed in our earlier study on selective electro-

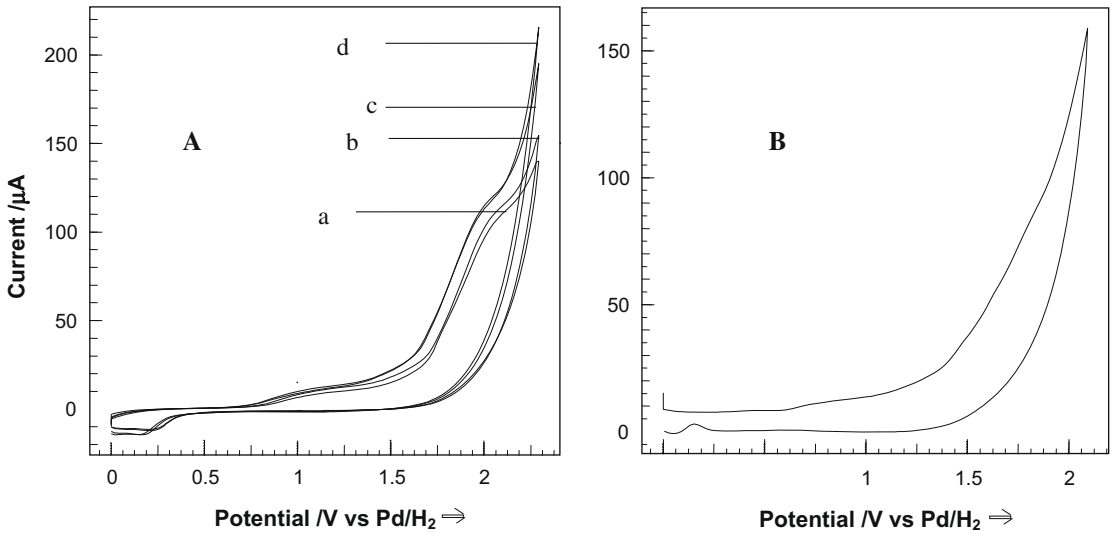

Fig. 1. A. Cyclic voltammograms for a platinum electrode in $Et_3N \cdot 4HF$ containing 20 (a), 30 (b), 40 (c) and 50 (d) mM of *N*-ethyl phenylacetamide (**1c**). Scan rate 20 mV/s. B. Cyclic voltammogram for a platinum electrode in neat $Et_3N \cdot 4HF$.

chemical fluorination of alkyl phenylacetates [21]. This is also in consistence with the earlier reports on the anodic fluorination of benzene, toluene and halo benzene in $R_4NF{\cdot}mHF$ medium [25–27].

From the chemical shift values, the presence of some cleaved products could also be identified and the ^{19}F NMR data corresponding to these products are summarized in Table 10.

3.4. Cyclic voltammetry and potentiostatic electrolysis

In our earlier work on the anodic fluorination of alkyl phenylacetates, high selectivity of side chain monofluoro derivative (87%) was observed under galvanostatic experimental conditions [21]. The results obtained for *N*-alkyl and *N*,*N*-dialkyl phenylacetamides presented above indicate low selectivity. Cyclic voltammetric as well as potentiostatic electrolysis experiments were carried out for these compounds to understand the reasons for such a poor selectivity.

Typical cyclic voltammograms for 30, 40, 50 and 60 mM of **1c** in $Et_3N \cdot 4HF$ medium on platinum and glassy carbon electrodes are presented in Figs. 1 and 2 along with the background current at a constant sweep rate of 20 mV/s. The oxidation peak for **1c** occurred in the background region (around 2.0 V) and hence no sharp anodic peak was noticed on the platinum electrode. On glassy carbon, however, a well defined oxidation peak was noticed at around 1.5 V which increased with increasing reactant concentration. Hence, further voltammetric studies were carried out on glassy carbon working electrode.

Typical cyclic voltammograms of **1c**, **6b**, **1e** and **6d** on glassy carbon electrode at a sweep rate of 20 mV/s are compared in Fig. 3. The anodic peak potentials for these four compounds are 1.50, 1.59, 1.60 and 1.74 V, respectively and the anodic peak current for **1c** is higher than **1e**. In general, *N*,*N*-dialkyl phenylacetamides showed higher anodic peak current when compared to their corresponding *N*-alkyl phenylacetamides. The cyclic voltammogram for **6d** indeed exhibited two peaks supporting this observation.

The above observations suggest that *N*,*N*-dialkyl phenylacetamides may undergo anodic fluorination in the adsorbed and non

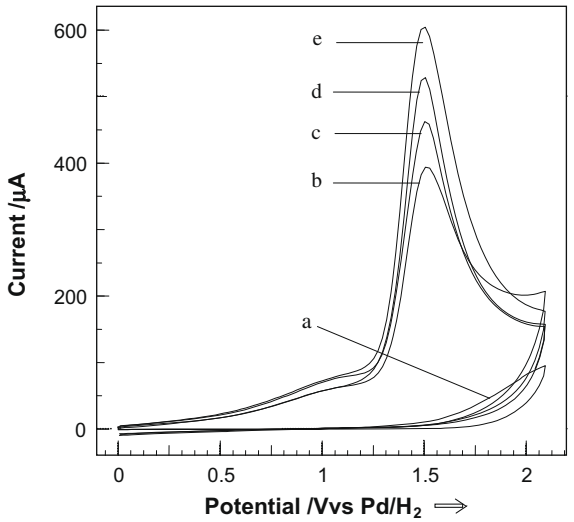

Fig. 2. Cyclic voltammograms for a Glassy carbon electrode in $Et_3N \cdot 4HF$ containing 0 (a), 30 (b), 40 (c), 50 (d) and 60 (e) mM of **1c**. Scan rate 20 mV/s.

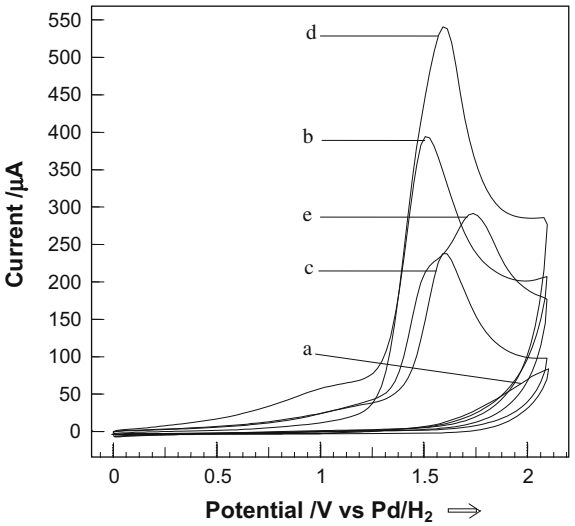

Fig. 3. Cyclic voltammograms for a Glassy carbon electrode in $Et_3N \cdot 4HF$ alone (a) and 30 mM **1c** (b), **1e** (c), **6b** (d) and **6d** (e) in the same medium. Scan rate 20 mV/s.

Table 12
Experimental conditions during the potentiostatic electrolysis of **1c** and **6b**.

Reactants	Concentration (mM)	Potential (V)	Time (min)	Cell voltage (V)	Charge (F/mole)	Current (mA)
1c	100	2.0	685	2.40–2.38	2	2.6–2.1
1c	100	2.2	67	2.63–2.60	2	26.0–23.0
1d	100	2.2	75	2.66–2.69	2	25.0–21.3
1e	100	2.2	90	2.67–2.72	2	22.5–18.7
6b	100	2.2	26	2.86–2.83	2	65.0–58.0

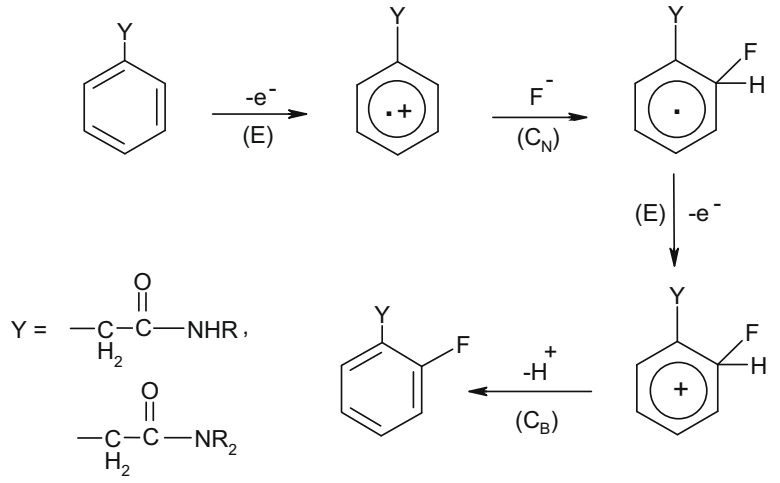

Scheme 4. EC_NEC_B mechanism of anodic fluorination.

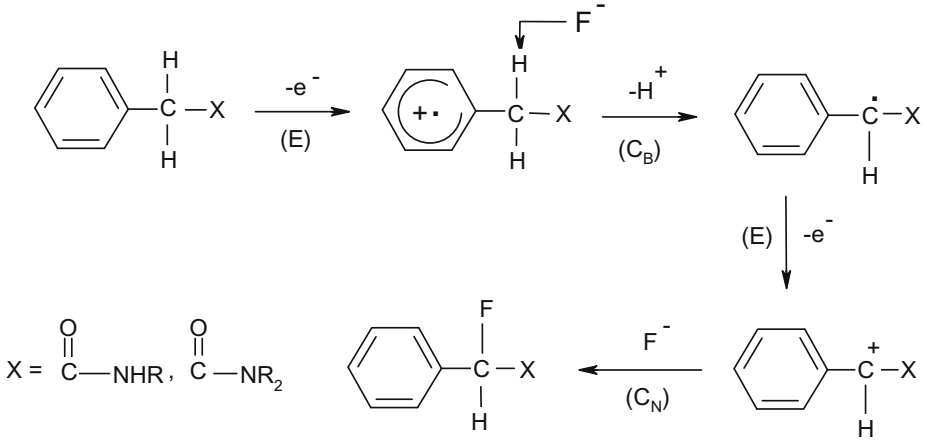

Scheme 5. EC_BEC_N mechanism of anodic fluorination.

adsorbed modes. The number of products formed and their distribution for *N*,*N*-dialkyl phenylacetamides are generally higher (Table 9) when compared to their corresponding *N*-alkyl phenylacetamides (Table 5).

Constant potential electrolysis was also carried out for **1c–e** and **6b** to understand the product distribution pattern between potentiostatic and galvanostatic electrolysis processes. The experimental conditions for potentiostatic electrolysis of these compounds are given in Table 12. When the potential for electrolysis was fixed at the peak potential E_{pa}, or at any other potential below 2.0 V, the electrolysis current was found to be extremely low and no fluorinated products were isolated or identified. The electrolysis proceeded smoothly at a constant potential of 2.0 and 2.2 V on platinum electrode and the cell voltage remained constant during electrolysis. Substantially higher current was noticed for **6b** when compared to **1c–e** at the same potential of 2.2 V. The product distribution obtained after the passage of 2 F/mol of electric charge under galvanostatic and potentiostatic conditions for **1c–e** are presented in Table 5 (compare run 3,5,7 and 4,6,8), respectively. Nuclear fluorination leading to **2c–e** was predominant under galvanostatic conditions while side chain fluorination **3c–e** was predominant under potentiostatic conditions (Table 5). In the case of **6b**, the side chain fluorination product (**7b**) was 26.1% under galvanostatic conditions and this product selectivity increased to

53.9% under potentiostatic conditions (run 2 and 3 in Table 9). Other side products were also generated under potentiostatic conditions and their yields were found to be low.

In a related work reported recently from this laboratory, high selectivity towards side chain fluorination at the active methylene group was obtained from alkyl phenyl acetates, even under galvanostatic conditions [21]. Under quiet similar galvanostatic conditions, *N*-alkyl and *N*,*N*-dialkyl phenylacetamides yielded nuclear *o*-fluorinated compound as the predominant products (Table 5 and 9). In $Et_3N \cdot 4HF$ medium it appears that acetamides undergo facile protonation [30,31].

It was also observed that the oxidation potentials of organic compounds depended on the electrode material. The anodic peak potential of *N*-ethyl phenylacetamide (**1c**) was nearly 0.5 V higher on platinum electrode when compared to glassy carbon electrode due to greater adsorption and blocking effects on platinum electrodes with increasing size and number of alkyl groups, which increased the number of multiple products. The fluorination of *N*,*N*-dialkyl phenylacetamides produced variety of products (Scheme 2) when compared to *N*-alkyl phenylacetamides (Scheme 1). Maximum selectivity of 54% of (2 F/mol) monofluoro active methylene derivative was obtained for *N*,*N*-diethyl phenylacetamide.

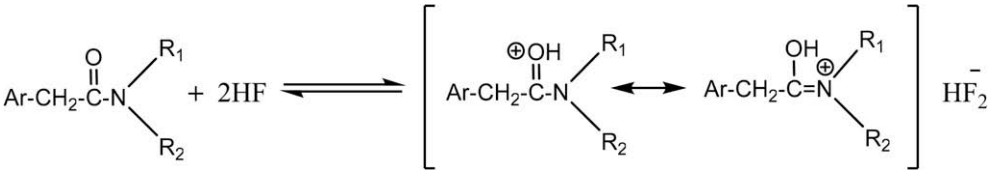

(1)

The direct oxidation of methylene group in the protonated species (**22**) would be more difficult. Hence this species undergoes oxidation at the aromatic nucleus leading to *o*-fluorinated product through EC_NEC_B mechanism (Scheme 4). The unprotonated species (**21**), on the other hand undergoes side chain oxidation at the active methylene group through EC_BEC_N mechanism (Scheme 5). Hence relatively more number of fluorinated products are obtained during the anodic fluorination of *N*-alkyl and *N*,*N*-dialkyl phenylacetamides when compared to alkyl phenylacetates reported earlier [21].

Under galvanostatic conditions, both the protonated and unprotonated species in Eq. (1) undergo simultaneous fluorination. Since protonated species (**22**) is likely to be in excess in $Et_3N \cdot 4HF$, nuclear fluorination predominates under galvanostatic conditions. Under potentiostatic conditions, however, the unprotonated species (**21**) would apparently undergo facile oxidation at lower oxidation potentials leading to more selectivity towards side chain fluorinated product. Even at constant potential conditions, formation of side products due to oxidative fluorination of adsorbed species are noticed to some extent. However, by selecting appropriate experimental conditions, selectivity upto 54% (2 F/mol) could be achieved for **6b** under potentiostatic electrolysis.

4. Conclusions

The present investigation indicated that $Et_3N \cdot nHF$ with an anodic potential limit of 2.0–2.2 V can be used as a fluorinating medium like $Et_4NF \cdot mHF$. If the oxidation potential of the reactant molecule is lower than the background limit as in the case of alkyl phenylacetates [21] good product selectivity can be achieved under galvanostatic conditions. On the other hand, if the oxidation potential of the reactant molecule is closer to the background limit, multiple product formation is possible under galvanostatic conditions. In such cases, electrolysis at constant potential conditions leads to improved product selectivity as observed in the case of *N*-alkyl and *N*,*N*-dialkyl phenylacetamides. The improved selectivity at constant potential conditions may be due to the selective oxidation of unprotonated reactant molecules at the side chain active methylene group.

Acknowledgements

The authors wish to thank the CSIR, New Delhi for granting SRF and J. Kennedy CECRI for taking GC/MS spectra.

References

[1] M. Noel, V. Suryanarayanan, S. Chellammal, J. Fluorine Chem. 83 (1997) 31–40.
[2] M. Noel, V. Suryanarayanan, J. Appl. Electrochem. 34 (2004) 357–369.
[3] T. Fuchigami, A. Konno, J. Syn. Org. Chem. Jpn. 55 (1997) 301–312.
[4] K.M. Dawood, Tetrahedron 60 (2004) 1435–1451.
[5] T. Fuchigami, J. Fluorine. Chem. 128 (2007) 311–316.
[6] F.G. Drakesmith, Top. Curr. Chem. 193 (1997) 197–242.
[7] K.M. Dawood, S. Higashiya, Y. Hou, T. Fuchigami, J. Org. Chem. 64 (1999) 7935–7939.
[8] S.M. Riyadh, H. Ishii, T. Fuchigami, Tetrahedron 57 (2001) 8817–8821.
[9] Y. Cao, T. Fuchigami, J. Electroanal. Chem. 587 (2006) 25–30.
[10] V. Suryanarayanan, M. Noel, J. Fluorine Chem. 92 (1998) 177–180.
[11] V. Suryanarayanan, S. Chellammal, M. Noel, J. Fluorine Chem. 93 (1999) 53–59.
[12] T. Fuchigami, T. Hayashi, K. Akinori, Tetrahedron Lett. 33 (1992) 3161–3164.
[13] E. Laurent, B. Marquet, R. Tardivel, F.R. 2604,189, 1990.
[14] S. Chebli, E. Laurent, B. Marquet, F.R. 2641,002, 1990.
[15] L. Kabore, S. Chebli, R. Faure, E. Laurent, B. Marquet, Tetrahedron Lett. 31 (1990) 3137–3140.
[16] C. Béguin, S. Hamman, L. Kaboré, E. Laurent, B. Marquet, J. Fluorine Chem. 58 (1992) 236.
[17] V. Dinoiu, T. Fukuhara, K. Miura, N. Yoneda, J. Fluorine Chem. 121 (2003) 227–231.
[18] B.A. Shainyan, Y.S. Danilevich, A.A. Grigoreva, Y.A. Chuvashevs, Russ. J. Org. Chem. 40 (2004) 513–517.
[19] L.S. Jalmes, J. Fluorine Chem. 127 (2006) 85–90.
[20] M.F. Greaney, W.B. Motherwell, Tetrahedron Lett. 41 (2000) 4467–4470.
[21] N. Ilayaraja, A. Manivel, D. Velayutham, M. Noel, J. Fluorine Chem. 129 (2008) 185–192.
[22] E. Laurent, B. Marquet, R. Tardivel, J. Fluorine Chem. 49 (1990) 115–126.
[23] S. Hara, S.Q. Chen, T. Hatakeyama, T. Fukuhara, M. Sekiguchi, N. Yoneda, Tetrahedron Lett. 36 (1995) 6511–6514.
[24] S.Q. Chen, T. Hatakeyama, T. Fukuhara, S. Hara, N. Yoneda, Electrochim. Acta 42 (1997) 1951–1960.
[25] K. Momota, M. Morita, Y. Matsuda, Electrochim. Acta 38 (1993) 1123–1130.
[26] K. Momota, K. Mukai, K. Kato, M. Morita, Electrochim. Acta 43 (1998) 2503–2514.
[27] K. Momota, T. Yonezawa, K. Mukai, M. Morita, J. Fluorine Chem. 87 (1998) 173–178.
[28] M. Hasegawa, T. Fuchigami, Electrochim. Acta 49 (2004) 3367–3372.
[29] T. Fuchigami, T. Tajima, J. Fluorine Chem. 126 (2005) 181–187.
[30] R.J. Gillespie, T. Birchall, Can. J. Chem. 41 (1963) 148–155.
[31] A.V. Purkina, A.I. Kol'tsov, B.Z. Volchek, J. Appl. Spectrosc. 15 (1971) 1051–1057.